ELSEVIER

Chemical etching characteristics for cellulose nitrate

C.W.Y. Yip, D. Nikezic [1], J.P.Y. Ho, K.N. Yu [*]

Department of Physics and Materials Science, City University of Hong Kong, Tat Chee Avenue, Kowloon Tong, Kowloon, Hong Kong, PR China

Abstract

Cellulose nitrate films (commercially available as LR 115 films were irradiated systematically with alpha particles in the energy range from 1 to 5 MeV with incident angles from $30°$ to $90°$. After etching to remove a thickness of 6.5 μm, the lengths of the major and minor axes of the alpha-particle track openings in the films were measured with an image analyser under an optical magnification of 10^3. These data were used altogether to derive a V function (ratio between the track etch rate and the bulk etch rate), which took the functional form of the Durrani–Green's function, i.e., $V = 1 + (a_1 \exp(-a_2 R') + a_3 \exp(-a_4 R'))(1 - \exp(-a_5 R'))$, but with new constants as $a_1 = 2.14$, $a_2 = 0.12$, $a_3 = 2.7$ and $a_4 = 0.135$ ($a_5 = 1$). We then went on to correct for the different etched thickness for different datasets. With these corrections, the experimental data were found to fit the model very satisfactorily. It was also interesting to see that the range of the calculated etched layer was consistent with the expected range.
© 2005 Published by Elsevier B.V.

Keywords: Cellulose nitrate; Irradiation effects; Radiation damage; Chemical etching

1. Introduction

Cellulose nitrate films (commercially available as LR 115 films from DOSIRAD, France) have been commonly used as solid-state nuclear track detectors (SSNTDs) in which visible tracks can be formed after ion irradiation and suitable chemical etching. Recent reviews on SSNTDs can be found in Ref. [1] and on ion tracks in Ref. [2]. Ion-track growth in SSNTDs has been suggested to base on two parameters, V_t and V_b [3], where V_t is the track etch rate (i.e., the rate of chemical etching along the ion trajectory) and V_b is the bulk etch rate (i.e., the rate of chemical etching of the undamaged surface). Over the years, many models have been developed [4–10]. Recently, the tracks were considered as three-dimensional objects [11], which enabled calculations of the track parameters including the lengths of the major and minor axes of track openings, and plotting of their profiles [12,13]. Although the track growth models have been developed for more than 30 years, comparisons between the values calculated from the track growth models with experimental values of track parameters for various incident angles and energies of the ions have been scarce. In most cases, comparisons have been limited to normal incidence, or only the critical angles have been measured. For example, Dorschel et al. [14] found good agreements between calculated and measured track parameters, but only considering the incident angle of $40°$.

In the present work, we compare experimental data on the lengths of major and minor axes of the track openings in LR 115 films with the values calculated from our three-dimensional model [11]. This comparison enables determination of the V function for the LR 115 films.

2. Experimental methodology

LR 115 films consist of thin films of cellulose nitrate manufactured by DOSIRAD, France. Type 2 non-strippable LR 115 films, with a 12 μm thick sensitive (or active) cellulose nitrate layer coated on a 100 μm thick polyester base, were employed in the present studies. The active layers of these films were systematically irradiated with alpha

---

[*] Corresponding author. Tel.: +852 27887812; fax: +852 27887830.
  E-mail address: peter.yu@cityu.edu.hk (K.N. Yu).
[1] On leave from Faculty of Sciences, University of Kragujevac, Serbia and Monte Negro.

particles from an ^{241}Am alpha particle source (main initial energy $E_0 = 5.48$ MeV) through a collimator made of acrylic resin with a hole diameter of 3 mm. By using air as the stopping medium between the source and the films, the incident alpha energies on the films ranged from 1 to 5 MeV, with steps of 0.5 MeV. The incident alpha particle energies were determined with an alpha spectroscopy system (ORTEC Model 5030). The incident angle was also varied from 30° up to 90°, with steps of 10°. For each chosen incident angle, a special procedure has been taken to irradiate different parts of the active layer of the same LR 115 film by alpha particles with different energies. This procedure ensures a uniform active layer thickness after chemical etching for all incident alpha energies for each incident angle.

The irradiated films were etched in standard etching conditions usually utilized for LR 115, i.e., in a 2.5N NaOH solution at 60°, until the remaining active-layer thickness was 5.5 μm, which was used in our previous studies [12]. However, it is noted that the bulk etch rate varies drastically with the amount of stirring, which means that the etched thickness of the active layer cannot be controlled solely by the temperature and concentration of the etchant, and the duration of etching [15]. Continuous monitoring of the remaining active-layer thickness is required. In the present work, this thickness was non-destructively monitored using energy dispersive X-ray fluorescence (EDXRF) [16]. Other techniques of non-destructive monitoring of the active-layer thickness of the LR 115 film are also available [17,18].

The lengths of the major and minor axes of track openings were measured by an Image Processing and Analysis System (Leica Imaging Systems QWin standard V2.3) with a magnification of 1000. More than 20 tracks were measured and analysed for each combination of incident energy and angle.

In this way, the experimental dataset consists of a total of 126 data, 63 for the major axis and 63 for the minor axis, for 9 incident energies and 7 incident angles (although the data for the major and minor axes are identical for normal incidence). Here, all the tracks observed in the LR 115 films were taken into account, regardless of whether they perforated the sensitive layer or not.

3. Results and the *V* function

The experimental results for the lengths of the major axis D_{exp} and the minor axis d_{exp} of track openings are shown as solid circles in Figs. 1 and 2, respectively. The error bars represent the standard deviations of the investigated 20 tracks. Along with these, the lengths for the major axis D_{calc} and the minor axis d_{calc} were calculated for the same irradiation

conditions used in the experiments. As mentioned above, our track growth model [11] was employed for the calculations. Input parameters in the model included the incident energy and angle of the alpha particle, etching time, V_b and the V_t function. The input energy was used to calculate the range of the corresponding alpha particles in cellulose nitrate, which was accomplished using the SRIM program [19] (the cellulose nitrate film has the chemical composition $C_6H_8O_9N_2$ and a density $\rho = 1.4$ g cm^{-3}, which were entered into the SRIM program).

The ratio $V(R') = V_t(R')/V_b$ could also be used, where R' was the residual range of the particles. The V function given by Durrani and Green [20] was adopted in the present work (hereafter referred to as the Durrani and Green function):

$$V = 1 + (a_1 e^{-a_2 R'} + a_3 e^{-a_4 R'})(1 - e^{-a_5 R'}) \qquad (1)$$

in a modified form. Originally, the constants for the function in Eq. (1) were given by Durrani and Green [20] as

$$a_1 = 100, \qquad a_2 = 0.446, \qquad a_3 = 4,$$
$$a_4 = 0.044, \qquad a_5 = 1 \qquad (2)$$

We systematically adjusted the constants a_k ($k = 1$ to 4) in Eq. (1) to obtain the best agreement with our experimental dataset (a total of 126 data for D_{exp} and d_{exp} as mentioned above), through minimization of N which was defined as

$$N = \sum_{i=1}^{7} N_i = \sum_{i=1}^{7} \sum_{j=1}^{9} \left\{ \sqrt{\left[D_{exp}(i,j) - D_{calc}(i,j)\right]^2 + \left[d_{exp}(i,j) - d_{calc}(i,j)\right]^2} \right\} \qquad (3)$$

where summation was performed for 7 incident angles (with the index i), and for 9 incident energies (with the index j). The constant a_1 was changed from 1 to 10, with steps of 0.5, the constant a_2 from 0.1 to 1 with steps of 0.1, a_3 from 1.5 to 3 with steps of 0.1 and finally a_4 from 0.04 to 0.14 with steps of 0.02. For each combination of constants, D_{calc} and d_{calc} were calculated for all incident angles and energies.

With the variation of the constants a_k, N showed some oscillatory behavior. When the first run with the ranges and steps given above was finished and the best combination (where N was smallest) was found, the second run was performed varying the constants about best values obtained in the first run, with much smaller steps. This procedure was repeated several times in order to find the combination of constants that gave the smallest N. In this way we found the best combination of constants as

$$a_1 = 2.14, \qquad a_2 = 0.12, \qquad a_3 = 2.7,$$
$$a_4 = 0.135 \qquad (4)$$

The results of calculations using this set of constants a_k are shown as dotted curves in Fig. 1 for the major axes and in Fig. 2 for the minor axes.
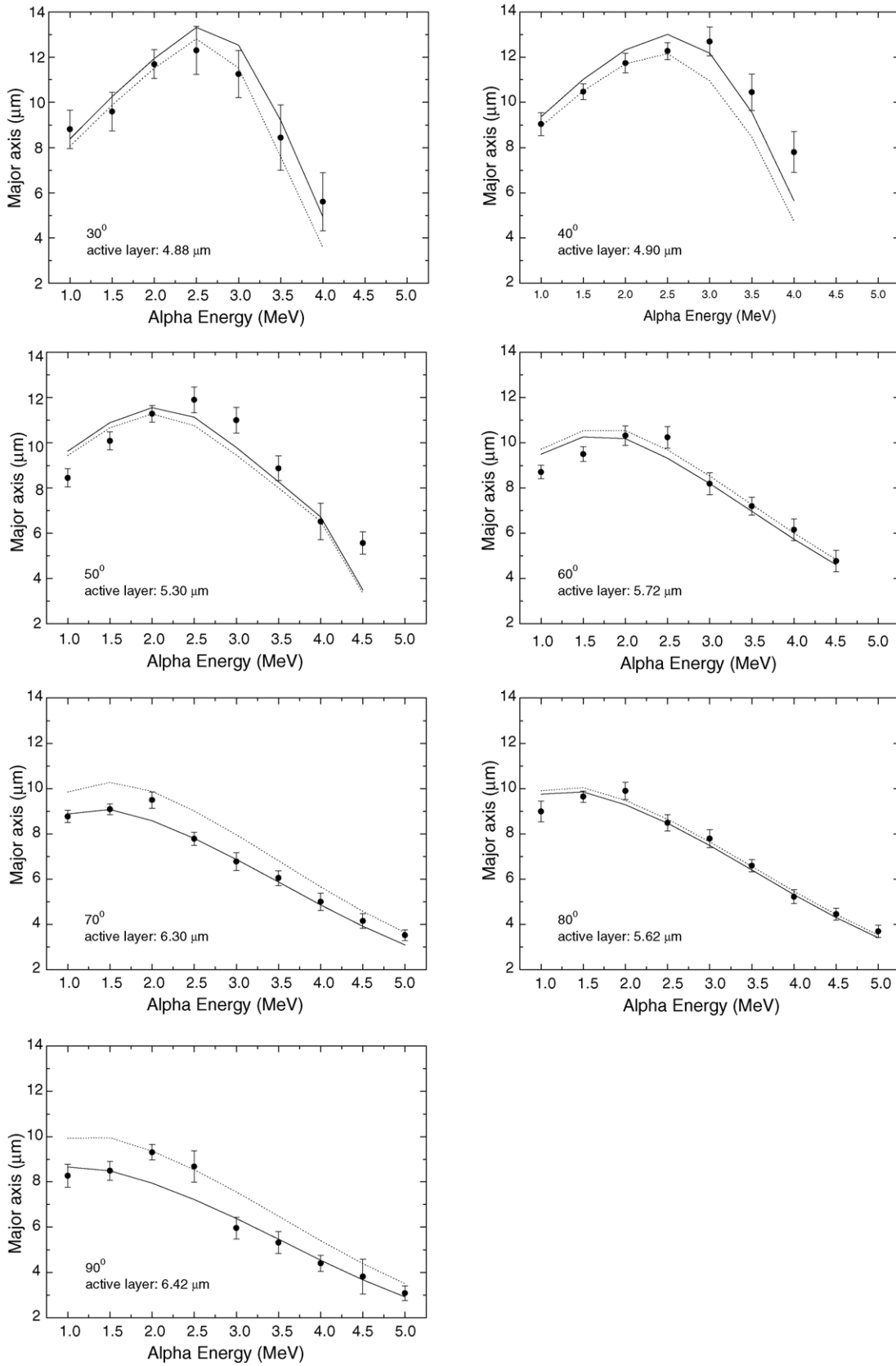
Fig. 1. Lengths of the major axis of track openings in the LR 115 film from alpha particles with different incident energies and incident angles. Solid circles: experimental data (with the error bars showing the standard deviations); dotted lines: calculated values for a remaining active-layer of 5.5 μm; Solid lines: calculated values for the remaining active-layer shown in the insert.
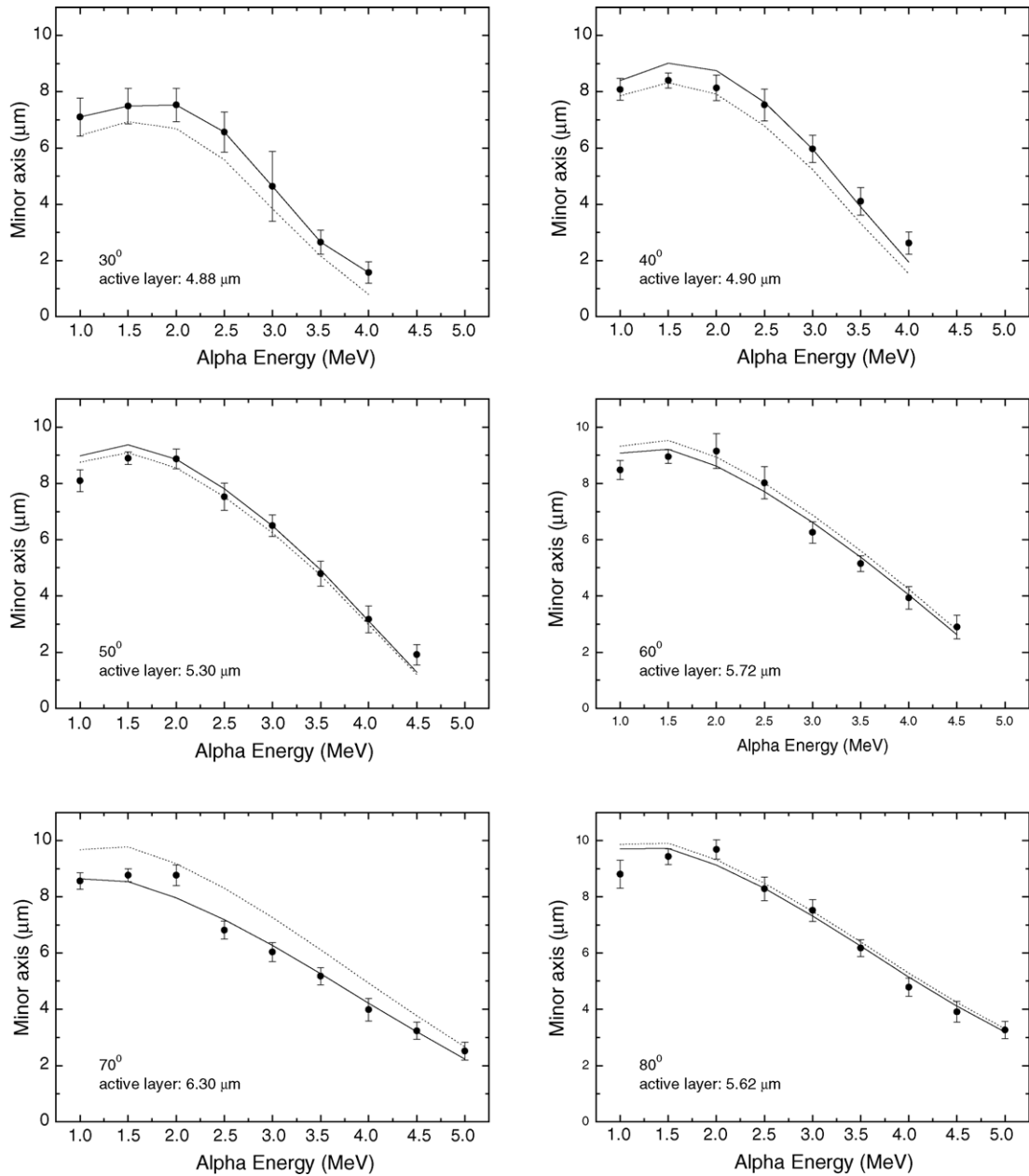
Fig. 2. Lengths of the minor axis of track openings in the LR 115 film from alpha particles with different incident energies and incident angles. Solid circles: experimental data (with the error bars showing the standard deviations); dotted lines: calculated values for a remaining active-layer of 5.5 μm; Solid lines: calculated values for the remaining active-layer shown in the insert.

4. Corrections for the remaining active layer thicknesses

From Figs. 1 and 2, we can see that, except for the incident angles of 50°, 60° and 80°, there are some systematic discrepancies between the experimental results and the calculated values. For incident angles of 30° and 40°, the calculated values are systematically lower than the experimental results, while for incident angles of 70° and 90°, the calculated values are systematically higher than the experimental results. It is interesting to observe that the trends of the discrepancies are the same for both the major and minor axes. These

observations suggest the possibility of a different remaining active-layer thickness from the nominal value of 5.5 μm.

Although the thickness of the active layer was monitored in the present work using EDXRF [16], the uncertainty was estimated to be around 1 μm at the thickness of about 5.5 μm, which was mainly due to the uncertainty in measuring the EDXRF intensities. Therefore, we expected the remaining active layer thickness in our experiments to range from 4.5 to 6.5 μm.

Our next task was therefore to correct for the different remaining active-layer thickness for datasets for different incident angles. By using the newly established a_k values
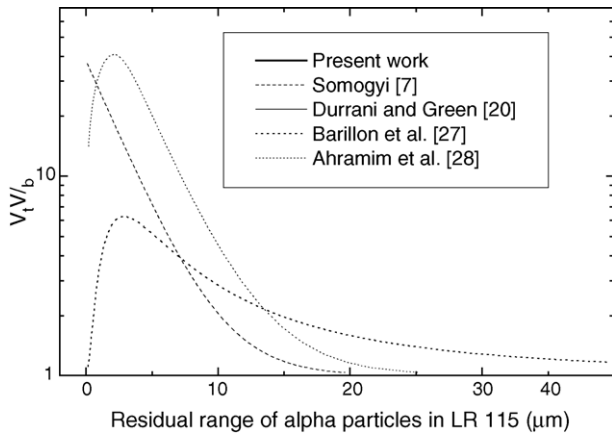
Fig. 3. The V function (=V_t/V_b) from the present work, and those from previous investigations.

given in Eq. (4), we minimized the value of N_i for the dataset for the i-th incident angle to obtain the corresponding remaining active-layer thickness. The fits to the experimental data after corrections for the remaining active-layer thicknesses are shown as solid lines in Figs. 1 and 2, and the corrected remaining active-layer thicknesses are shown as inserts in the figures. It can be seen that the experimental data are now fitted by the model very satisfactorily. It is also interesting to see that the corrected remaining active-layer thicknesses range from 4.88 to 6.42 μm, which is consistent with the expected range of 4.5–6.5 μm mentioned above.

5. Discussion about the V function

Recently, a method for determining the V_t function in polyallyldiglycol carbonate (CR-39) was proposed by Dorschel et al. [21]. The CR-39 detectors were polished from the side and the track lengths were then measured from the lateral view of the tracks. This method brought many new results. For example, for some light ions (^{4}N, ^{16}O), the V function for CR-39 was found to be not only a function of the residual range, but also to depend on the position inside the detector [22], which was referred to as the "depth dependence" of V although it also depended on the initial ion energy. This finding was confirmed by other research groups and for other ions (Li, C) [23]. The effect was more pronounced if the ion was heavier. This method has not been applied to the LR 115 film until now. Other recent developments in the determination of the V function include the use of the confocal microscope [24] and surface profilometry [25]. However, results were given only for the CR-39.

A few V functions for alpha particles in cellulose nitrate have been published. The function from Durrani and Green [20] given in Eq. (1) with the original constants listed in Eq. (2) is shown in Fig. 3. A maximum appears close to the end of the particle range, which corresponds to the Bragg peak in the stopping power curve. The maximum is very high, with $V_{max} \approx 45$. A nominal $V_b \approx 3.3\ \mu m\ h^{-1}$ [26] will give $V_t \approx 150\ \mu m\ h^{-1}$, which may be too high. For example, according to SRIM, the range of alpha particles with energy of 2.5 MeV is 11.8 μm. By evaluating $\int_0^{11.8} dx/V_t(R'-x)$, one may show that such tracks take only about 28 min of etching to perforate the sensitive layer. Another 20 min of etching will be needed to obtain visible tracks when the bottom of the tracks achieves the diameter in the order of 1 μm. Therefore, the total time needed to obtain visible tracks is about 50 min, which is only half the time elapsed when the first track appears according to Barillon et al. [27].

Barillon et al. [27] also published a V function for alpha tracks in LR 115 in the form

$$V_t = V_b + \frac{1}{a_1^2 + \left[a_2 R' - \frac{1}{a_3 R'}\right]^2} \tag{5}$$

with constants $a_1 = 0.23$, $a_2 = 0.032$, and $a_3 = 3.8$. In the same paper, they also tried a V_t function which was proportional to the ionizing rate I, i.e., $V_t = KI$, where K was a proportionality constant, and they concluded that this approach was unsuccessful because of the lack of information between the process of physical energy loss and creation of damages in the material that were responsible for the etching process. The function in Eq. (5) is shown in Fig. 3.

Another function also based on the proportionality between V_t and the ionizing rate I was proposed by Aharmim et al. [28] in the form

$$V_t = V_b + I(R')e^{-\eta R'} \tag{6}$$

where $I(R')$ was the ionizing rate as a function of the residual range obtained from the SRIM program, and η was determined to be 0.281. Eq. (6) was also programmed and the results are given in Fig. 3. Some minor differences from the original data given by Aharmim et al. were observed, which were due to the different density of cellulose nitrate taken here as 1.4 g cm^{-3} [29] instead of 1.52 [28].

Somogyi [7] proposed a V function in the form

$$V = 1 + e^{-aR'+b} \tag{7}$$

with constants $a = 0.356$ and $b = 3.611$.

All functions mentioned above [7,20,27,28] were programmed and plotted in Fig. 3 for comparisons. In the low-energy region, there are large discrepancies among the functions, with the Durrani–Green's function [20] and the function of Ahmarim et al. [28] on one side, and with the function of Barillon et al. [27] on the other. The maximum of the function of Barillon et al. is about eight times lower than those for the function of Durrani and Green and that of Ahmarim et al. In the region of larger residual ranges, i.e., above 20 μm, the function of Barillon et al. converges to that of Durrani and Green, while that of Aharmim et al. drops to unity much faster. Somogyi's function is below that of Barillon et al. for residual ranges above 8 μm and is closer to the Durrani and Green's function for smaller residual ranges.

This function is also the steepest one, which drops to unity at a residual range of about 20 μm. In contrast to other *V* functions, Somogyi's function does not show any maximum close to the end of the particle range.

The function given in Eq. (1) with the constants listed in Eq. (4), which are determined in this work, is also shown in Fig. 3 together with the original Durrani and Green's function as well as other functions mentioned above. A large difference is observed between the original Durrani and Green's function and the one found in the present work. The discrepancy is very pronounced in the low-energy region around the Bragg peak, at which our function is about 10 times smaller than the original one. At larger residual ranges, these two functions converge. Our function is the closest to the function of Barillon et al. The difference is significant in the low-residual-range region, and the two functions are almost parallel in other regions. The functions of Somogyi and Ahramim et al. are very different from ours, for all values of the residual range.

6. Conclusions

In this paper, LR 115 cellulose nitrate films were systematically irradiated with alpha particles with incident energies from 1 to 5 MeV and incident angles from 30° to 90°. After etching in a 2.5N NaOH solution kept at 60° to achieve a nominal remaining active-layer thickness of 5.5 μm, the lengths of major and minor axes of the alpha-track openings were measured. These data were used altogether to derive a *V* function for the LR 115 film, which took the functional form of the Durrani–Green's function but with new constants. We then went on to correct for the different remaining active-layer thickness for different datasets. With these corrections, the experimental data were fitted by the model very satisfactorily. It is also interesting to see that the range of the calculated remaining active layer thicknesses is consistent with the expected range.

Acknowledgment

References

[1] D. Nikezic, K.N. Yu, Mater. Sci. Eng. R 46 (2004) 51.
[2] R.L. Fleisher, Ion tracks, in: J.H. Westbrook, R.L. Fleischer (Eds.), Intermetallic Compounds Principles and Practice, vol. 3, John Wiley, 2002, p. 263.
[3] R.L. Fleisher, P.B. Price, R.M. Walker, Nuclear Track in Solids. Principles and Applications, University of California Press, Berkley, 1975.
[4] R.P. Henke, E.V. Benton, Nucl. Instr. Meth. 97 (1971) 483.
[5] H.G. Paretzke, E.V. Benton, R.P. Henke, Nucl. Instr. Meth. 108 (1973) 73.
[6] G. Somogyi, S.A. Szalay, Nucl. Instr. Meth. 109 (1973) 211.
[7] G. Somogyi, Nucl. Instr. Meth. 173 (1980) 21.
[8] M. Fromm, P. Meyer, A. Chambaudet, Nucl. Instr. Meth. B 107 (1996) 337.
[9] U. Hatzialekou, D.L. Henshaw, A.P. Fews, Nucl. Instr. Meth. A 263 (1988) 504.
[10] P. Meyer, M. Fromm, A. Chambaudet, J. Laugier, L. Makovicka, Radiat. Meas. 25 (1995) 449.
[11] D. Nikezic, K.N. Yu, Radiat. Meas. 37 (2003) 39.
[12] D. Nikezic, K.N. Yu, Nucl. Instr. Meth. B 196 (2002) 105.
[13] D. Nikezic, K.N. Yu, Radiat. Meas. 37 (2003) 595.
[14] B. Dorschel, D. Hermsdorf, U. Reichelt, S. Starke, Y. Wang, Radiat. Meas. 37 (2003) 563.
[15] C.W.Y. Yip, J.P.Y. Ho, V.S.Y. Koo, D. Nikezic, K.N. Yu, Radiat. Meas. 37 (2003) 197.
[16] C.W.Y. Yip, J.P.Y. Ho, D. Nikezic, K.N. Yu, Radiat. Meas. 36 (2003) 161.
[17] F.M.F. Ng, C.W.Y. Yip, J.P.Y. Ho, D. Nikezic, K.N. Yu, Radiat. Meas. 38 (2003) 1.
[18] K.N. Yu, F.M.F. Ng, Nucl. Instr. Meth. B 226 (2004) 365.
[19] J.F. Ziegler, 2001. SRIM-2000 (http://www.srim.org/).
[20] S.A. Durrani, P.F. Green, Nucl. Tracks 8 (1984) 21.
[21] B. Dorschel, H. Hartmann, K. Kadner, Radiat. Meas. 26 (1996) 51.
[22] B. Dorschel, D. Hermsdorf, S. Starke, Radiat. Meas. 37 (2003) 583.
[23] M. Fromm, F. Vaginay, G. Meesen, A. Chambaudet, A. Poffijn, Radiat. Meas. 36 (2003) 93.
[24] F. Vaginay, M. Fromm, D. Pusset, G. Meesen, A. Chambaudet, A. Poffijn, Radiat. Meas. 34 (2001) 123.
[25] K.N. Yu, F.M.F. Ng, J.P.Y. Ho, C.W.Y. Yip, D. Nikezic, Radiat. Protect. Dosimetry 111 (2004) 93.
[26] D. Nikezic, A. Janicijevic, Appl. Radiat. Isotop. 57 (2002) 275.
[27] R. Barillon, M. Fromm, A. Chambaudet, H. Marah, A. Sabir, Radiat. Meas. 28 (1997) 619.
[28] B. Aharmim, A. Sabir, H. Marah, Radiat. Meas. 35 (2002) 307.
[29] S.A. Durrani, R.K. Bull, Solid State Nuclear Track Detection. Principles Methods and Applications, Pergamon Press, Oxford, 1987.